

On the Origin of Asymmetric Induction of the Palladium-Catalyzed Allylic Substitution Reaction with Chiral 4,4-Disubstituted 4,5-Dihydro-2-(phosphinoaryl)oxazole Ligands

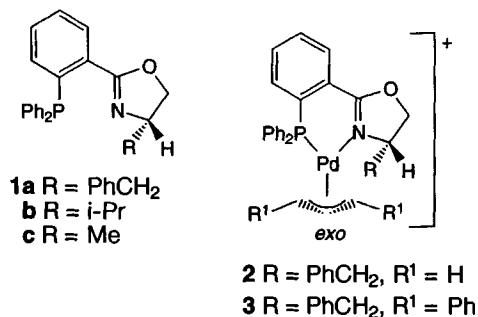
by Silvia Schaffner, Jürgen F. K. Müller, Markus Neuburger, and Margareta Zehnder*

Institut für Anorganische Chemie der Universität Basel, Spitalstrasse 51, CH-4056 Basel

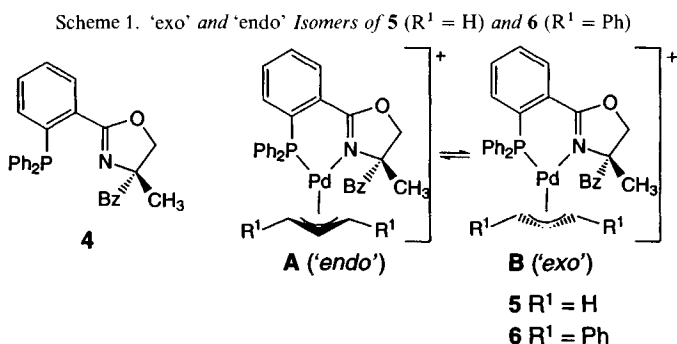
The X-ray analyses of $(\eta^3\text{-allyl})\{\text{4-benzyl-2-[2-(diphenylphosphino-}\kappa\text{P)phenyl]-4,5-dihydro-4-methyloxazole-}\kappa\text{N}\}$ palladium(II) hexafluorophosphate (**5**) and the analogous $[\text{Pd}(\eta^3\text{-1,3-diphenylallyl})]$ complex **6** are presented. A comparison with the $(\eta^3\text{-allyl})$ - and $(\eta\text{-1,3-diphenylallyl})$ palladium complexes **2** and **3**, respectively, containing the 4-monosubstituted 4,5-dihydro-2-(phosphinoaryl)oxazole ligand **1a** reveals important structural differences (Fig. 3). $^1\text{H-NMR}$ Spectroscopic investigations confirm that the 4,4-disubstituted 4,5-dihydro-2-(phosphinoaryl)oxazole ligand **4** of **5** and **6** shows the same conformation in solution as in the solid state (Table 2). The application of ligand (*S*)-**4** in the Pd-catalyzed allylic substitution demonstrates a configurational relationship between the orientation of the allyl ligand in the intermediate (*cf.* complex **6**) and the absolute configuration of the allylic-substitution product (Table 3).

Introduction. – The importance of the Pd-catalyzed allylic substitution reaction with chiral dihydro(phosphinoaryl)oxazole ligands **1** as a versatile synthetic method for enantioselective C–C bond formations [1] initiated controversial discussions about its mechanism [2]. Recently, some of the intermediates occurring in the catalytic cycle were investigated. Their structures were determined in the solid state as well as in solution [2b, f][3]. First assumptions about an early transition state [2b, e] are now in contrast to observations made by us that the low ee values in the substitution reaction of $[\text{Pd}(\eta^3\text{-MeCHCHCHMe})]$ complexes with a chiral dihydro(phosphinoaryl)oxazole ligand correspond to the formation of at least four different cationic $(\eta^3\text{-1,3-dimethylallyl})$ -[dihydro(phosphinoaryl)oxazole]palladium(1+) isomers [3d]. Independently, a NMR study by Helmchen and coworkers provided reliable evidence for a $[\text{Pd}^0(\text{olefin})]$ complex, which favors more a late transition state [2f].

To gain deeper insight into the configuration-determining step, we now investigated the influence of a second alkyl substituent in α -position (C(4)) to the N-atom of the



dihydrooxazole moiety on the geometry of the (η^3 -allyl)[dihydro(phosphinoaryl)oxazole]-palladium(1+) cation. Coordinated 4-monosubstituted dihydro(phosphinoaryl)oxazole ligands such as in **2** and **3** usually show a very rigid conformation [2b][3][4]. Previous results have already demonstrated that the allyl ligand of such complexes might adopt 'exo' or 'endo' orientations of the central allylic proton with respect to the larger substituent at C(4) of the dihydrooxazole moiety. Therefore, we expected a strong influence of the presence of a second alkyl substituent at C(4) on the 'exo'/'endo' ratio of the allylic moiety. To examine this influence, the 4,4-disubstituted 4,5-dihydro-2-(phosphinoaryl)-oxazole ligand **4** was prepared, and the solution and X-ray structures of its complexes (see **5** and **6**) were determined and compared. Furthermore, a correlation with the catalytic activity of these novel complexes was established.



'exo': The central C–H bond of the allyl group points towards the larger substituent at C(4) (Bz); 'endo': the central C–H bond points away from the larger substituent.

Results and Discussion. – X-Ray analyses of $[Pd^{II}(\eta^3-C_3H_5)(4)]PF_6$ (**5**) and of $[Pd^{II}(\eta^3-PhC_3H_3Ph)(4)]PF_6$ (**6**) were carried out. Selected geometric parameters are reported in Table 1. For numbering, see Figs. 1 and 2.

Table 1. Selected Geometrical Parameters [\AA , $^\circ$] with e.s.d.'s in Parentheses for **5** and **6** and Comparison with the Data of **3**

	5a	5b	5c	6	3
Pd(1)–N(1)	2.110(4)	2.103(4)	2.108(4)	2.155(6)	2.101(6)
Pd(1)–P(1)	2.261(1)	2.269(1)	2.255(1)	2.282(2)	2.281(2)
Pd(1)–C(100)	2.101(5)	2.076(6)	2.073(6)	2.121(8)	2.149(7)
Pd(1)–C(200)	2.142(6)	2.168(9)	2.169(7)	2.220(6)	2.177(9)
Pd(1)–C(201)		2.169(9)	2.18(2)		
Pd(1)–C(300)	2.219(6)	2.246(5)	2.250(6)	2.376(7)	2.266(1)
C(100)–C(200)	1.376(9)	1.32(1)	1.313(9)	1.41(1)	1.41(1)
C(100)–C(201)		1.32(1)	1.35(1)		
C(200)–C(300)	1.358(9)	1.33(1)	1.350(9)	1.40(1)	1.39(1)
C(201)–C(300)		1.34(1)	1.31(1)		
Interplanar angles:					
(allyl)/Pd–P–N	118.9	119.7 117.5	121.8 120.6	111.7	117.6
Pd–C(100)–C(300)/Pd–P–N	6.2	0.9	1.0	23.5	12.5

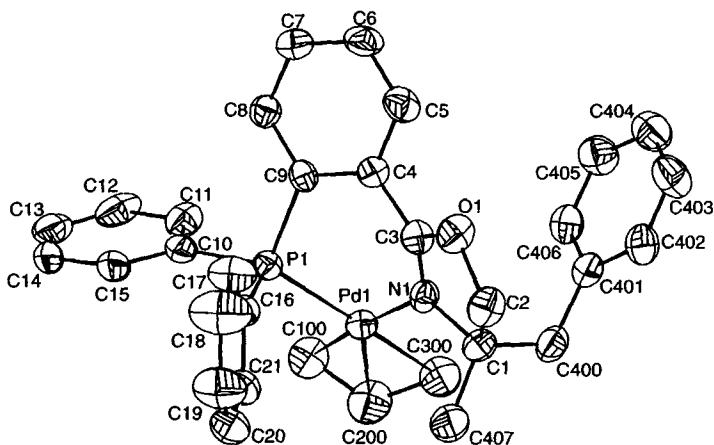


Fig. 1. X-Ray structure of complex **5a**. Thermal ellipsoids are drawn at 30% probability.

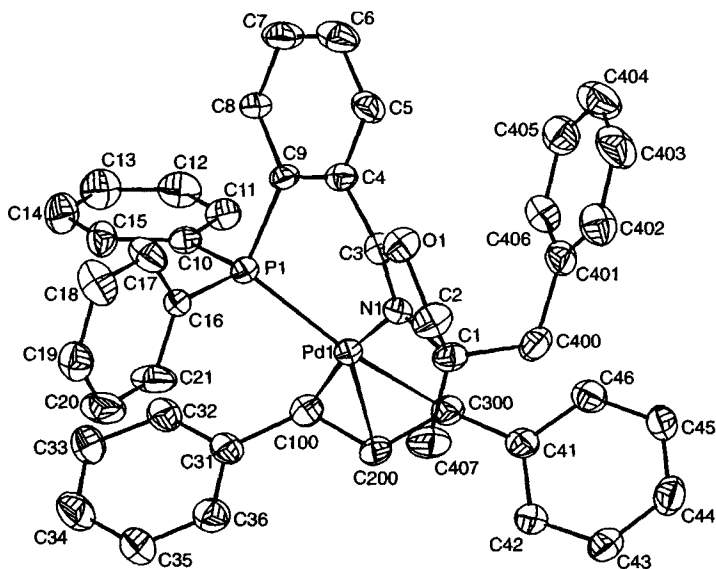


Fig. 2. X-Ray structure of complex **6**. Thermal ellipsoids are drawn at 30% probability.

Crystal Structure of 5. Crystals of **5** have three crystallographically independent formula units per asymmetric unit. For clarity, only **5a** is depicted in Fig. 1. The coordination geometry of the three cations **5a–c** is pseudo-square-planar. Bond lengths and bond angles are in the expected range (Table 1). The cations differ in the orientation of the allyl group. Cation **5a** has the ‘endo’ configuration. The allyl ligand of **5b** is disordered. A refinement of the crystallographic occupancy factors afforded an ‘endo’/‘exo’ ratio of 54:46. Cation **5c** also shows disorder. The ‘endo’/‘exo’ ratio is 79:21. It seems that disorder of the allyl group is common for $[\text{Pd}^{\text{II}}(\eta^3\text{-C}_3\text{H}_5)]$ compounds. In all previ-

ously determined crystal structures of $[\text{Pd}^{\text{II}}(\eta^3\text{-C}_3\text{H}_5)(\mathbf{1})]\text{PF}_6$ salts with chiral dihydro(phosphinoaryl)oxazoles, an 'endo'/'exo' disorder was observed in the solid state [2b][3a–c].

Crystal Structure of 6. In **6**, the interaction between the Ph group of the allyl ligand and the more demanding dihydrooxazole moiety leads to a considerable distortion of the square planar coordination geometry as compared to that of **5** and **3** (see Table 1). The Pd–C distance to the allylic terminus *cis* to the oxazole moiety (2.376(7) Å) is 0.110 Å longer than the corresponding distance in **3** (2.266(10) Å). The Pd–P–N plane forms an angle of 23.5° with the Pd–C(100)–C(300) plane. Thus, the coordination geometry lies between the square-planar structure of a $[\text{Pd}^{\text{II}}(\pi\text{-allyl})]$ and the trigonal geometry of a $[\text{Pd}^0(\text{olefin})]$ complex.

The essential features of the dihydro(phosphinoaryl)oxazole backbone of ligand **4** in **5** and **6** are very similar. Due to the non-planarity of the chelate ring, one *P*-phenyl group of **4** adopts a pseudoaxial and the other a pseudoequatorial position (Fig. 3, a). The benzyl group of **4** is equatorially positioned with respect to the Pd–P–N plane and lies on the opposite side of the coordination plane to the axial *P*-phenyl group. Surprisingly, the dihydro(phosphinoaryl)oxazole ligand adopts the inverse conformation compared with the 4-monosubstituted ligands of type **1** (Fig. 3, b).

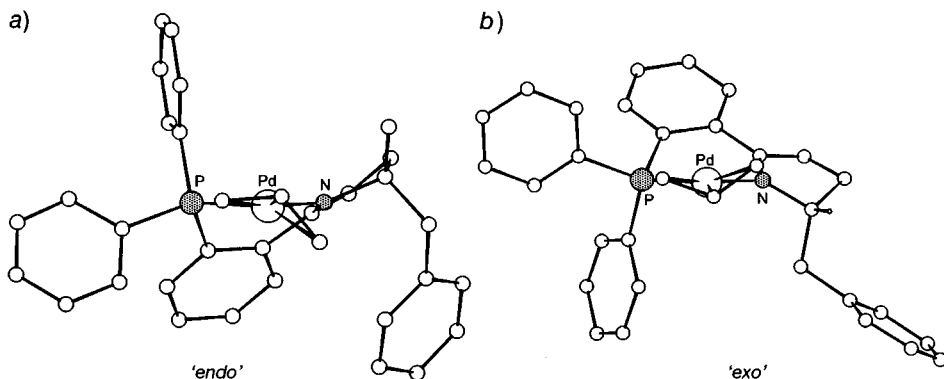


Fig. 3. a) $[\text{Pd}(\eta^3\text{-PhC}_3\text{H}_3\text{Ph})(\mathbf{4})]$ (**6**) in the 'endo' configuration and b) $[\text{Pd}(\eta^3\text{-Ph-C}_3\text{H}_3\text{-Ph})(\mathbf{1a})]$ (**3**) in the 'exo' configuration. The Ph groups of the allyl ligand are omitted for clarity.

The allyl ligand of **6** adopts exclusively the 'endo' configuration. This is in contrast with the $[\text{Pd}^{\text{II}}(\eta^3\text{-PhC}_3\text{H}_3\text{Ph})(\mathbf{1})]$ complexes which are always 'exo'-configured in the solid state. However, with respect to the phosphine moiety, the allyl ligand is oriented in the same way as in complex **3** (Fig. 3). The closest interligand distance (3.30(1) Å) is found between the allyl substituent and the equatorial Ph group at the P-atom. It is assumed that minimization of the interligand interaction at the phosphine side of the complex is the reason for the preference of 'endo' isomer **A**. This is in agreement with the studies of Pregosin and Albinati [5]. They found that an arrangement of the PPh_2 moiety and the Ph group at the allyl ligand in which the central proton of the allyl moiety and the pseudoaxial *P*-phenyl group are oriented in the same direction is sterically favored.

¹H-NMR Spectroscopy. The ¹H-NMR data of the allylic protons are summarized in Table 2. The ¹H-NMR spectrum of **5** shows two sets of slightly broadened signals at room temperature, indicating an exchange process between form **A** ('endo') and **B** ('exo'). The diastereoisomer ratio is *ca.* 55:45. Almost the same 'endo'/'exo' ratio was also found in [Pd^{II}(η³-C₃H₅)(**1**)] complexes.

Table 2. Selected ¹H-NMR Data (δ in ppm, J(H,H), J(H,P) in Hz) of **5** and **6**

	δ (H)			
	5 major	5 minor	6 major	6 minor
H _{anti} -C(100) ^a)	2.96 (<i>J</i> = 11.3)	3.16 (<i>J</i> = 12.2)	4.33 (<i>J</i> = 9.3)	4.59 (<i>J</i> = 11.1)
H _{syn} -C(100) ^a)	3.54 (<i>J</i> = 6.6)	3.52 (<i>J</i> = 6.6)		
H-C(200)	5.84 ^c)	5.84 ^c)	6.76 ^c)	6.70
H _{anti} -C(300) ^a)	3.65 (<i>J</i> = 14.0, 10.4)	3.96 (<i>J</i> = 13.9, 10.5)	6.28 (<i>J</i> = 14.4, 9.7)	6.3 ^c)
H _{anti} -C(300) ^a) ^b)	2.51	3.92	6.05	5.05
H _{syn} -C(300) ^a)	5.07 (<i>J</i> ≈ 6.9)	4.96 (<i>J</i> ≈ 7.0)		

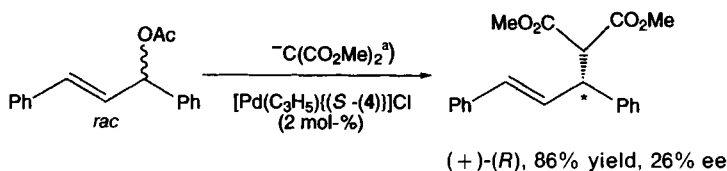
^a) *anti* or *syn* configuration with respect to the central proton H-C(200). ^b) Chemical shifts of the corresponding 4-monosubstituted complexes. ^c) Data incomplete due to signal overlap.

The NMR spectrum of **6** reveals that a mixture of two isomers in a 75:25 ratio is present in solution. According to the H,H coupling constants of the allylic protons, the Ph substituents are in the *syn* position with respect to the central proton. No evidence for the presence of *syn-anti* isomers was obtained.

The ¹H-NMR data of **5** and **6** suggest that the dihydro(phosphinoaryl)oxazole adopts the same conformation in solution as in the solid state. This suggestion is derived from prior ¹H-NMR investigations of compounds **2** and **3** [3a]. In these complexes, the shielding effect of the Ph ring of the benzyl substituent shifts the H_{anti}-C(300) resonances of the 'endo' isomers by *ca.* 1 ppm to higher field relative to the corresponding signals of the 'exo' isomers¹⁾. In contrast, in **5** and **6**, no shielding effect is observed. This suggests that the benzyl group is equatorially positioned, and an interaction between its Ph ring and the allyl group is not possible (Fig. 3, a).

Catalysis. Asymmetric allylic substitution of 1,3-diphenylprop-2-enyl acetate with dimethyl malonate was carried out using the catalyst (*S*)-**4** and following the previously

Scheme 2



^a) H₂C(COOMe)₂ (3 equiv.), BSA (3 equiv.), KOAc (2 mol-%), CH₂Cl₂, 23°

¹⁾ X-Ray analyses of [Pd(η³-allyl)(**1a**)] complexes reveal that the benzyl ligand may adopt both, a position outside of the coordination sphere (complexes **2** and **3** [3a]) or above the allyl moiety ([Pd(η³-MeC₃H₃Me)(**1a**)] [3d]).

described procedure with *N,O*-bis(trimethylsilyl)acetamide (BSA) under the same conditions as with ligands **1** (Scheme 2) [6]. The enantiomeric excess (ee) and absolute configuration were determined by chiral HPLC and optical-rotation measurements [7].

The results listed in Table 3 demonstrate a relationship between the orientation of the allyl ligand and the product of the substitution reaction. With catalyst (*S*)-**4** (cf. complex **6**), the major product has the reversed (+)-(*R*) configuration as compared to the major allylic substitution product obtained in the presence of ligands of type (*S*)-**1** (\rightarrow (–)-(*S*) configuration). The different asymmetric induction is attributed to the flip of the dihydro(phosphinoaryl)oxazole backbone as well as to the 'endo' orientation of the allyl ligand in complex **6**. A correlation of the configuration of the $[\text{Pd}(\eta^3\text{-PhC}_3\text{H}_3\text{Ph})]$ moiety and the configuration of the product was also reported by Togni *et al.* in allylic aminations with [(diphenylphosphino)ferrocenyl]pyrazole catalysts [8]. In this case, the inversion of the asymmetric induction was based on the formation of *syn-syn* and *syn-anti* isomers, respectively.

Table 3. Diastereoisomer Ratio of $[\text{Pd}(\pi\text{-allyl})]$ Complexes vs. Asymmetric Induction

$[\text{Pd}(\eta^3\text{-Ph-C}_3\text{H}_3\text{-Ph})(\text{L})]\text{PF}_6$			Catalysis		
L	diastereoisomer ratio (de) [%]	Config. of the allyl ligand (major diastereoisomer)	ee [%]	Abs. config. of product	Ref.
(<i>S</i>)- 1a	85:15 (70)	' <i>exo</i> '	97	(–)-(<i>S</i>)	[1]
(<i>S</i>)- 1b	87:13 (74)	' <i>exo</i> '	98	(–)-(<i>S</i>)	[1]
(<i>S</i>)- 1c	80:20 (60)	' <i>exo</i> '	89	(–)-(<i>S</i>)	[1]
(<i>S</i>)- 4	75:25 (50)	' <i>endo</i> '	26	(+)-(<i>R</i>)	

However, the ratio of the two isomers is not directly correlated with the asymmetric induction. In our case, (*S*)-**4** led to a substantially lower asymmetric induction and to a longer reaction time than catalysts of type **1**. The stereochemical course of the reaction may be rationalized by a mechanism for enantioselection similar to that proposed by Brown *et al.* for 1-[2-(diphenylphosphino)-1-naphthyl]isoquinoline ligands [2d]. The preferred nucleophilic attack at the allyl terminus *trans* to the P-atom of the predominant diastereoisomer leads to a product-like geometry. In the reaction with catalysts of type **1**, the nucleophilic addition at the allylic intermediate relieves the steric strain (Fig. 4, a).

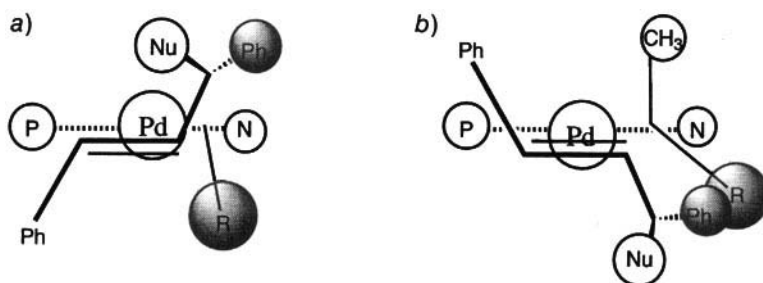


Fig. 4. Olefinic product complex with a) ligand **1** and b) ligand **4**

In contrast, with ligand **4** the nucleophilic attack leads to a sterically more hindered addition product (Fig. 4, b).

Conclusion. – In enantioselective catalysis, mechanistic interpretations concerning the origin of the asymmetric induction usually focus on the chiral sense of the applied auxiliary. The related diastereotopic transition states are then assumed to be responsible for the enantioselective discrimination. In our case, this interpretation is somewhat misleading, as chirality is a property of a molecule as a whole and not focused at a single chirality center. The change of the whole chiral shape in the intermediate complex (cf. **6**) obviously has a crucial influence on the absolute configuration of the obtained main stereoisomer. We initiated a switch of the chiral shape of the intermediate complex by introducing a second alkyl substituent at C(4) of the dihydro(phosphinoaryl)oxazole ligand (see **4**) compared with the monosubstituted ligands **1** (cf. [Pd(π -allyl)(**1**)] complexes **2** and **3**) without changing the absolute configuration of the dihydrooxazole moiety. Although the relative orientation of the allyl ligand to the dihydro(phosphinoaryl)-oxazole backbone was maintained, an 'endo' orientation was found in the main isomer of **6**. These changes are responsible for the reversed configuration of the main stereoisomer produced upon allylic substitution in the presence of ligand (*S*)-**4** in comparison with the ligands (*S*)-**1a–c** containing a monosubstituted dihydrooxazole moiety. The nucleophilic attack on the allylic terminus has to occur *trans* to the P-atom to release steric strain. But the introduction of the second alkyl substituent induces additional steric strain. This is expressed in the reduced enantioselectivity and reactivity of the palladium complex (*S*)-**6** derived from ligand (*S*)-**4**.

The support of this project by the *Swiss National Science Foundation* (project No. 21-45/276.95) is gratefully acknowledged.

Experimental Part

General. The preparation of 2-(diphenylphosphino)benzonitrile has been detailed in [3a]. Commercially available solvents and reagents were used without further purification, except for those detailed below. CH₂Cl₂ was distilled over CaH₂ under Ar. Solvents for chromatography were distilled before use. (\pm)- α -Methylphenylalanine and (*S*)- α -methylphenylalanine were purchased from *Bachem*, purity > 99%. Moisture- and air-sensitive reactions were carried out under N₂ using dried glassware. Column chromatography (CC): SiO₂, *C* 560, 0.035–0.070 mm, *F* 254, *Chemische Fabrik, Uetikon*. Optical rotation: 10-cm cell at 20°; *Perkin-Elmer-141* polarimeter. NMR Spectra: *Varian-Gemini 300*; ¹H, 300 MHz, CDCl₃, chemical shifts δ in ppm vs. SiMe₄ (= 0 ppm), coupling constants *J* in Hz; ³¹P, 121 MHz, triphenyl phosphate as external reference (–18.0 ppm).

(\pm)- α -Methylphenylalaninol [9]. To a stirred suspension of NaBH₄ (1.00 g, 25 mmol) in THF (10 ml), α -methylphenylalanine (1.80 g, 10 mmol) was added. After stirring for 1 h, the mixture was immersed in an ice bath, and a soln. of conc. H₂SO₄ (0.66 ml, 25 mmol) in Et₂O (1.5 ml) was added dropwise. The stirring was continued at r.t. overnight. MeOH (1.5 ml) and 5*N* NaOH (5 ml) were successively added. After removal of the org. solvents, the aq. mixture was refluxed for 2 h. The aq. soln. was extracted with CH₂Cl₂ (4 \times 10 ml). Evaporation yielded α -methylphenylalaninol (1.47 g, 89%). Colorless oil which solidified upon standing. ¹H-NMR: 7.18–7.34 (*m*, 5 arom. H); 3.36 (*d*, *J* = 10.6, 1 H, CCH₂OH); 3.32 (*d*, *J* = 10.6, 1 H, CCH₂OH); 2.70 (*s*, PhCH₂); 1.65–1.95 (*br. s*, OH, NH₂); 1.04 (*s*, Me).

(*S*)- α -Methylphenylalaninol. As described above with NaBH₄ (0.50 g, 12.5 mmol) and (*S*)- α -methylphenylalanine (0.90 g, 10 mmol) of 0.72 g (87%) of (*S*)- α -methylphenylalaninol. Colorless solid.

(\pm)-4-Benzyl-2-[2-(diphenylphosphino)phenyl]-4,5-dihydro-4-methyloxazole (**4**) [10]. A stirred suspension of 2-(diphenylphosphino)benzonitrile (0.91 g, 3.17 mmol), (\pm)- α -methylphenylalaninol (0.62 g, 3.75 mmol), and ZnCl₂ (0.50 g, 3.68 mmol) in chlorobenzene (7 ml) under N₂ was heated to reflux for 72 h. The mixture was submitted to CC (4 \times 5 cm, silica gel). The unreacted benzonitrile was removed with CH₂Cl₂ (100 ml). The

[ZnCl₂(4)] complex was eluted with AcOEt (150 ml). This zinc complex (1.44 g, 80%) was dissolved in CHCl₃ (5 ml) and treated with an equimolar amount of 2,2'-bipyridine (0.39 g, 2.52 mmol) in CHCl₃ (5 ml). The resulting white suspension was stirred for 1 h and then submitted to CC (4 × 5 cm, silica gel, CHCl₃ (150 ml)): 0.88 g (80%) of 4. Colorless oil. ¹H-NMR: 7.76–7.80 (m, 1 arom. H); 7.10–7.33 (m, 17 arom. H); 6.80–6.84 (m, 1 arom. H); 4.03 (d, *J* = 8.2, 1 H, CH₂); 3.51 (d, *J* = 8.2, 1 H, CH₂); 2.70 (d, *J* = 13.5, 1 H, PhCH₂); 2.59 (d, *J* = 13.5, 1 H, PhCH₂); 1.02 (s, Me). ³¹P-NMR: –4.79.

(*S*)-4-Benzyl-2-[2-(diphenylphosphino)phenyl]-4,5-dihydro-4-methyloxazole ((*S*)-4). As described for 4, with 2-(diphenylphosphino)benzonitrile (0.82 g, 2.85 mmol) and (*S*)-α-methylphenylalaninol (0.50 g, 3.03 mmol): 1.29 g (79%) of the intermediate Zn compound. Yield of (*S*)-4: 0.86 g (88%) of colorless solid.

(η³-Allyl){4-benzyl-2-[2-(diphenylphosphino-κP)phenyl]-4,5-dihydro-4-methyloxazole-κN}palladium(II) Hexafluorophosphate (5). A mixture of [PdCl(η³-allyl)]₂ (36 mg, 0.10 mmol) and of 4 (92 mg, 0.21 mmol) was stirred in EtOH (10 ml) for 15 min. The resulting soln. was treated with NH₄PF₆ (50 mg). After 10 min, the precipitate (62 mg) was filtered off. The filtrate was allowed to stand overnight. A second crop of crystalline solid (48 mg) precipitated: 110 mg (75%) of colorless crystals. Recrystallizing from CH₂Cl₂/EtOH/hexane 1:3:3 afforded air-stable crystals suitable for X-ray analysis. ¹H-NMR (for numbering, see Fig. 1): major isomer (55%): 6.95–7.69 (m, 19 arom. H); 5.84–5.98 (m, H–C(200)); 5.07 (br. ddd, H_{syn}–C(300)); 4.59 (d, *J* = 9.1, H–C(2)); 3.84 (d, *J* = 9.1, H–C(2)); 3.64 (dd, *J* = 10.4, 14.0, H_{anti}–C(300)); 3.54 (d, *J* = 6.6, H_{syn}–C(100)); 2.96 (d, *J* = 11.3, H_{anti}–C(100)); 2.92 (d, *J* = 13.6, H–C(400)); 2.78 (d, *J* = 13.6, H–C(400)); 1.30 (s, Me); minor isomer (45%): 6.95–7.73 (m, 19 arom. H); 5.84–5.98 (m, H–C(200)); 4.96 (br. ddd, H_{syn}–C(300)); 4.50 (d, *J* = 9.0, H–C(2)); 3.93 (d, *J* = 9.3, H–C(2)); 3.96 (dd, *J* = 10.5, 13.9, H_{anti}–C(300)); 3.52 (d, *J* = 6.6, H_{syn}–C(100)); 3.16 (d, *J* = 12.2, H_{anti}–C(100)); 2.86 (d, *J* = 13.9, H–C(400)); 2.76 (d, *J* = 13.9, H–C(400)); 1.30 (s, Me). ³¹P-NMR: 23.08 (major), 22.92 (minor).

{4-Benzyl-2-[2-(diphenylphosphino-κP)phenyl]-4,5-dihydro-4-methyloxazole-κN}(η³-1,3-diphenylallyl)palladium(II) Hexafluorophosphate (6). As described for 5, with [(η³-Ph₂C₃H₃)PdCl]₂ (65 mg, 0.098 mmol), and 4 (92 mg, 0.211 mmol): 141 mg (82%) of 6. Yellow crystals. ¹H-NMR (for numbering, see Fig. 2): major isomer (75%): 7.80–7.82 (m, 1 arom. H); 6.90–7.57 (m, 27 arom. H); 6.76 (dd, *J* ≈ 14.0, H–C(200)); 6.72–6.80 (m, 1 arom. H); 6.28 (dd, *J* = 9.7, 14.4, H_{anti}–C(300)); 4.33 (d, *J* ≈ 9.3, H_{anti}–C(100)); 4.27 (d, *J* = 9.1, H–C(2)); 3.36 (d, *J* = 9.1, H–C(2)); 1.87 (d, *J* = 13.5, H–C(400)); 1.75 (d, *J* = 13.5, H–C(400)); 1.26 (s, Me); minor isomer (25%): 7.62–7.68 (m, 1 arom. H); 6.90–7.57 (m, 27 arom. H); 6.70 (m, H–C(200)); 6.72–6.80 (m, 1 arom. H); 6.28 (dd, H_{anti}–C(300)); 4.59 (d, *J* ≈ 11.1, H_{anti}–C(100)); 4.02 (d, *J* = 9.0, H–C(2)); 3.58 (d, *J* = 9.0, H–C(2)); 2.57 (d, *J* = 13.0, H–C(400)); 2.11 (d, *J* = 13.0, H–C(400)); 0.85 (s, Me). ³¹P-NMR: 25.24 (major), 25.40 (minor).

Palladium-Catalyzed Allylic Alkylation Using the BSA Procedure. A mixture of [PdCl(C₃H₅)₂] (2.32 mg, 6.36 μmol) and (*S*)-4 (7 mg, 15.9 μmol, 1.25 equiv./Pd) in CH₂Cl₂ (0.6 ml) was stirred for 15 min at r.t. To the resulting pale yellow mixture, a soln. of *rac*-1,3-diphenylprop-2-enyl acetate (160.1 mg, 0.635 mmol) in CH₂Cl₂ (2 ml) was added. Then dimethyl malonate (252 mg, 1.9 mmol), *N,O*-bis(trimethylsilyl)acetamide (388 mg, 1.90 mmol), and KOAc (1.1 mg) were added. The mixture was stirred at r.t. for 22 h. Only traces of diphenylprop-2-enyl acetate were detected by TLC (hexane/AcOEt 3:1; *R*_f (starting material) 0.47, *R*_f (product) 0.37). The soln. was diluted with Et₂O (25 ml) and washed twice with ice-cold sat. aq. NH₄Cl soln. The org. phase was dried (Na₂SO₄) and evaporated. CC (SiO₂, hexane/AcOEt 3:1) afforded 181 mg (88%) of colorless (*E*)-2-(1,3-diphenylprop-2-enyl)propanedioic acid dimethyl ester. [α]_D²⁰ = + 5.53 (CHCl₃, *c* = 1.54); 26% ee of (*R*)-enantiomer, as measured on a Daicel Chiralcel OD column (λ 254 nm; hexane/*i*-PrOH 99:1, flow rate 0.3 ml/min; *t*_R 38.40 (*R*), 40.88 (*S*) min). ¹H-NMR (CDCl₃, 300 MHz): 7.19–7.32 (m, 10 arom. H); 6.49 (d, *J* = 15.6, H–C(3)); 6.33 (dd, *J* = 8.4, 15.8, H–C(2)); 4.27 (dd, *J* = 8.4, 10.7, H–C(1)); 3.95 (d, *J* = 10.8, H–C(2)); 3.70 (s, Me); 3.51 (s, Me).

*X-Ray Structure Analyses*²⁾. Crystal data and parameters of the data collection are compiled in Table 4. Unit-cell parameters were determined by accurate centering of 25 strong reflections. Reflection intensities were collected on a four-circle diffractometer (Enraf-Nonius CAD4). Three standard reflections were monitored every hour during data collection. The usual corrections were applied. The absorption correction was determined using φ -scans [11]. The structures were solved by direct methods [12]. Anisotropic least-squares refinement on *F* was

²⁾ Crystallographic data (excluding structure factors) for the structures reported in this paper have been deposited with the Cambridge Crystallographic Data Centre as deposition No. CCDC-101162. Copies of the data can be obtained, free of charge, on application to the CCDC, 12 Union Road, Cambridge CB2 1EZ, UK (fax: + 44 (1223) 336 033; e-mail: deposit@ccdc.cam.ac.uk).

Table 4. *Experimental Conditions for the X-Ray Analysis of 5 and 6*

	5	6
Chemical formula	C ₃₂ H ₃₁ F ₆ NOP ₂ Pd	C ₄₄ H ₃₉ F ₆ NOP ₂ Pd
Molecular weight	727.94	880.14
Crystal size [mm]	0.16 × 0.19 × 0.40	0.08 × 0.12 × 0.25
<i>a</i> [Å]	9.923(2)	11.151(2)
<i>b</i> [Å]	50.132(6)	16.168(6)
<i>c</i> [Å]	19.339(2)	22.547(2)
β [°]	91.72(1)	102.05(1)
<i>V</i> [Å ³]	9615(2)	3975(2)
Crystal system	monoclinic	monoclinic
Space group	<i>P</i> 2 ₁ / <i>n</i>	Cc
<i>Z</i>	12	4
<i>F</i> (000)	4416	1792
Radiation	CuK α (λ = 1.54180 Å)	CuK α (λ = 1.54180 Å)
Temperature [K]	293	293
Calc. density [g/cm ³]	1.51	1.47
Abs. coeff. [mm ⁻¹]	6.28	5.17
Scan type	$\omega/2\theta$	$\omega/2\theta$
θ_{\max} [°]	77.50	77.50
No of meas. refl.	17031	3987
No. of indep. refl.	16048	3943
No. of refl. in ref. $I \geq 3\sigma(I)$	12345	3377
No. of parameters	1271	509
Extinction	56.3(2.0)	51.2(5.9)
Final <i>R</i>	4.60	4.02
Final <i>R</i> _w	4.33	4.18
last max./min. in diff. map	0.61/–0.59	0.57/–0.48
Weighting scheme	Chebyshev polynomial [15]	

carried out on all non-H-atoms using the program 'CRYSTALS' [13]. Isotropic refinement was carried out on the allylic protons of **6**. The C–H distances were fixed to 0.96 Å. Positions of the remaining H-atoms were calculated. Scattering factors were taken from the International Tables of Crystallography, Vol. IV. *Figs. 1–3* were designed with the programme SNOOPI [14]. In **5**, two anions and the allyl group of **5b** and **5c** were found to be disordered. The disordered atoms were refined in two positions holding the sum of their occupancies equal to one. Geometric restraints were applied to the disordered parts of the structure during the structure refinement.

REFERENCES

- [1] P. von Matt, A. Pfaltz, *Angew. Chem.* **1993**, *105*, 614; *ibid.*, *Int. Ed. Engl.* **1993**, *32*, 566; P. von Matt, Ph. D. Thesis, University of Basel, 1993; J. Sprinz, G. Helmchen, *Tetrahedron Lett.* **1993**, *34*, 1769; G. J. Dawson, C. G. Frost, J. M. J. Williams, S. J. Coote, *ibid.* **1993**, *34*, 3149.
- [2] a) O. Reiser, *Angew. Chem.* **1993**, *105*, 576; *ibid.*, *Int. Ed. Engl.* **1993**, *32*, 547; b) J. Sprinz, M. Kiefer, G. Helmchen, M. Reggelin, G. Huttner, O. Walter, L. Zsolnay, *Tetrahedron Lett.* **1994**, *35*, 1523; c) J. V. Allen, S. J. Coote, G. J. Dawson, Ch. G. Frost, Ch. J. Martin, J. M. J. Williams, *J. Chem. Soc., Perkin Trans. 1* **1994**, 2065; d) J. M. Brown, D. I. Hulmes, P. J. Guiry, *Tetrahedron* **1994**, *50*, 4493; e) G. Helmchen, S. Kudis, P. Sennhenn, H. Steinhagen, *Pure Appl. Chem.* **1997**, *69*, 513; f) H. Steinhagen, M. Reggelin, G. Helmchen, *Angew. Chem., Int. Ed. Engl.* **1997**, *36*, 2108.
- [3] a) N. Baltzer, L. Macko, S. Schaffner, M. Zehnder, *Helv. Chim. Acta* **1996**, *79*, 803; b) L. Macko, Ph. D. Thesis, University of Basel, 1996; c) S. Schaffner, L. Macko, M. Neuburger, M. Zehnder, *Helv. Chim. Acta* **1997**, *80*, 463; d) S. Liu, J. F. K. Müller, M. Neuburger, S. Schaffner, M. Zehnder, *J. Organomet. Chem.* **1997**, *549*, 283.

- [4] G. C. Lloyd-Jones, A. Pfaltz, *Angew. Chem.* **1995**, *107*, 534; *ibid.*, *Int. Ed. Engl.* **1995**, *34*, 462; b) G. C. Lloyd-Jones, A. Pfaltz, *Z. Naturforsch., B* **1995**, *50*, 361.
- [5] P. Barbaro, P. S. Pregosin, R. Salzmänn, A. Albinati, R. W. Kunz, *Organometallics* **1995**, *14*, 5160.
- [6] U. Leutenegger, G. Umbricht, C. Fahrni, P. v. Matt, A. Pfaltz, *Tetrahedron* **1992**, *48*, 2143.
- [7] P. v. Matt, G. C. Lloyd-Jones, A. B. E. Minidis, A. Pfaltz, L. Macko, M. Neuburger, M. Zehnder, H. Rüegger, P. S. Pregosin, *Helv. Chim. Acta* **1995**, *78*, 265.
- [8] A. Togni, U. Burckhardt, V. Gramlich, P. S. Pregosin, R. Salzmänn, *J. Am. Chem. Soc.* **1996**, *118*, 1031.
- [9] A. Abiko, S. Masamune, *Tetrahedron Lett.* **1992**, *33*, 5517.
- [10] G. Koch, G. Lloyd-Jones, O. Loiseleur, A. Pfaltz, R. Prétôt, S. Schaffner, P. Schnyder, P. von Matt, *Recl. Trav. Chim. Pays-Bas* **1995**, *114*, 206.
- [11] A. C. T. North, D. C. Phillips, F. S. Mathews, *Acta Crystallogr., Sect. A* **1968**, *24*, 351.
- [12] A. Altomare, M. C. Burla, M. Camalli, G. Cascarano, C. Giacovazzo, A. Gualgliardi, G. Polidori, 'SIR92', *J. Appl. Crystallogr.* **1994**, *27*, 435.
- [13] D. Watkin, 'Crystals, Issue 9', Chemical Crystallography Laboratory, Oxford, 1990.
- [14] K. Davies, P. Braid, B. Foxman, H. Powell, 'SNOOPI', Oxford University, 1989.
- [15] J. R. Carruthers, D. J. Watkin, *Acta Crystallogr., Sect. A* **1979**, *35*, 698.

Received January 30, 1998